NANO EXPRESS

Open Access

CrossMark

Gas Transport Properties of Polybenzimidazole and Poly(Phenylene Oxide) Mixed Matrix Membranes Incorporated with PDA-Functionalised Titanate Nanotubes

V. Giel[*], M. Perchacz, J. Kredatusová and Z. Pientka

Abstract

Functionalised titanate nanotubes (TiNTs) were incorporated to poly(5,5-bisbenzimidazole-2,2-diyl-1,3-phenylene) (PBI) or poly(2,6-dimethyl-1,4-phenylene oxide) (PPO) for improving the interfacial compatibility between the polymer matrix and inorganic material and for altering the gas separation performance of the neat polymer membranes. Functionalisation consisted in oxidative polymerisation of dopamine-hydrochloride on the surface of non-functionalised TiNTs. Transmission electron microscopy (TEM) confirmed that a thin polydopamine (PDA) layer was created on the surface of TiNTs. 1.5, 3, 6, and 9 wt.% of PDA-functionalised TiNTs (PDA-TiNTs) were dispersed to each type of polymer matrix to create so-called mixed matrix membranes (MMMs). Infrared spectroscopy confirmed that –OH and –NH groups exist on the surface of PDA-TiNTs and that the nanotubes interact via H-bonding with PBI but not with PPO. The distribution of PDA-TiNTs in the MMMs was to some extent uniform as scanning electron microscope (SEM) studies showed. Beyond, PDA-TiNTs exhibit positive effect on gas transport properties, resulting in increased selectivities of MMMs. The addition of nanotubes caused a decrease in permeabilities but an increase in selectivities. It is shown that 9 wt.% of PDA-TiNTs in PBI gave a rise to CO_2/N_2 and CO_2/CH_4 selectivities of 112 and 63 %, respectively. In case of PPO-PDA-TiNT MMMs, CO_2/N_2 and CO_2/CH_4 selectivity increased about 25 and 17 %, respectively. Sorption measurement showed that the presence of PDA-TiNTs in PBI caused an increase in CO_2 sorption, whereas the influence on other gases is less noticeable.

Keywords: Polybenzimidazole, Poly(phenylene oxide), Titanate nanotubes, Polydopamine, Mixed matrix membrane, Gas separation, Permeability, Selectivity, Sorption isotherms

Background

Nanomaterials have attracted considerable interest in many applications, including the field of membrane science [1–7]. In the last decades, numerous works have been published on the use of inorganic particles in various polymeric membrane structures and their functionalities [1, 8–13]. The goal of such so-called mixed matrix membranes (MMMs) is to achieve a system with more useful structural or functional properties unattainable by any of the constituent itself which may help to overcome the efficiency-productivity trade-off of neat polymer materials [14].

Thus far, a wide range of nanoparticles were used in MMMs, e.g. zeolites, metal organic frameworks (MOFs), mesoporous silicas, carbon molecular sieves, or carbon nanotubes (CNTs) [9, 15–17]. The choice of nanoparticles for the desired gas separation is of greatest significance, because major variables as gas adsorption or molecular sieving abilities of the nanoparticles may seriously affect the MMM performance. Beyond, uniformly dispersed nanoparticles in the polymer matrix as well as interfacial bonding notably influence gas transport properties [9, 16, 18].

* Correspondence: giel@imc.cas.cz
Institute of Macromolecular Chemistry, Academy of Sciences of the Czech Republic, Heyrovsky Sq. 2, 16206 Prague 6, Czech Republic

Springer Open

Giel *et al. Nanoscale Research Letters* (2017) 12:3

Page 2 of 15

Hitherto, CNTs and their potential for MMMs have been studied in great detail and seems to be a prospective filler for overcoming the efficiency-productivity trade-off of neat polymer membranes because of their high aspect ratio [1, 19]. Several polymeric materials have been tested to prepare MMMs as shown later in the text to alter their gas separation characteristics. For example, Wang et al. has embedded multi-walled nanotubes (MWNT) into PEG-based Pebax solution to separate CO_2/CH_4 and CO_2/N_2, respectively [20]. Another study of Pebax membranes was performed by Murali et al. [21]. It was shown that MWNT in the Pebax matrix enhances substantially the permeability of H_2, O_2, CO_2, and N_2. Khan et al. incorporated pristine MWNTs into PIM-1, which caused as well an increase in gas permeabilities [12]. Rajabi et al. reported on the addition of functionalised MWNT to polyvinylchloride (PVC) membranes which resulted in better gas separation performance, especially for CO_2/CH_4 [22]. Studies by Kim and his group demonstrated that the permeabilities of O_2, N_2, and CH_4 increased proportionally to the amount of open-ended CNTs in the polymer matrix [23]. Li and his co-workers prepared MMMs from Matrimid and a combination of CNT and graphene oxide [24]. It was found that the MMMs with CNTs and graphene oxide had better gas separation performance than those with only one of these components, showing excellent separation properties. Cong et al. added single-walled carbon nanotubes (SWNT) and MWNT to brominated poly(2,6-dimethyl-1,4-phenylene oxide) (PPO) for CO_2/N_2 separation [25]. They observed that the MMMs had an increased CO_2 permeability, while the CO_2/N_2 selectivity remained the same. In addition, permeabilities increased with the content of CNT.

However, there are several drawbacks regarding the use of CNTs in MMMs [1, 19]: (1) extreme amount of energy consumption because of high process temperatures (1000–3700 °C); (2) expensive fabrication owing to lasers and inert atmosphere; and (3) additional purification steps necessary due to by-products. With respect to these major issues, the utilisation of new fillers in MMMs is desirable.

Hence, this work focuses on titanate nanotubes (TiNTs), a relatively new class of nanotubes made of non-carbon material. These nanotubes possess similar morphology as CNTs, but the synthesis is carried out at far lower temperatures and at low cost [26, 27]. Moreover, variations of TiNT compositions and structures may be practically unlimited and the possibility of functionalisation is a useful way of treatment that may improve adhesion to polymer matrices. To date, most research about TiNTs has been directed towards the efficient synthesis and functionalisation of this filler as well on investigation of its unique morphology and physico-

chemical properties [27–29]. However, almost all underlying studies about nanotubes for use in MMMs are connected to CNTs. Therefore, this study describes membranes altered by functionalised TiNTs and continues our earlier work in which and non-modified TiNTs were added to poly(5,5-bisbenzimidazole-2,2-diyl-1,3-phenylene) (PBI) or PPO [30]. Although various researches have been carried out on those polymers with diverse inorganic fillers, e.g. ZIF-8 [31], SBA-15 [32], silica nano particles [33, 34], there is so far no academic literature available on using functionalised TiNTs combined with PBI or PPO as membrane materials for gas separation, to the best of our knowledge. Therefore, the aim was to investigate the effect of TiNT on the gas transport properties of PPO and PBI membranes. It was found that the incorporation of non-modified TiNTs to PPO formed unselective voids, because the obtained ideal selectivities remained constant while permeabilities of all investigated gases increased. In case of PBI, the compatibility of non-modified TiNTs and the PBI matrix was enhanced because of the Ti–O groups present in TiNT which could interact with the N–H bonds present in PBI. These interactions increased the effective path of the penetrants, resulting in lower permeabilities and higher ideal selectivities.

Therefore, in continuation of this study [30], we attempted to functionalise the TiNTs in order to improve the adhesion between the filler and the polymer matrix, targeting to diminish the unselective voids and thus improving the membrane separation characteristics.

For the functionalisation was utilised polydopamine (PDA), because the formation of PDA layers onto nanotubes emerged as very efficient and facile [35–38]. Besides, PDA appears as a promising adhesive for subsequent surface-mediated reactions which allows tailoring properties according the used source materials [39, 40].

In the present work, the feasibility of the formation of MMMs based on PBI or PPO, respectively, and various amounts of PDA-TiNTs was studied. The as-prepared MMMs were characterised for their morphology, physicochemical properties, and gas separation performance, aiming to investigate the effect of PDA-TiNT content on PBI or PPO membranes.

Methods

Materials

The PPO powder was purchased from Spolana Neratovice (Czech Republic). For dissolving PPO chloroform (Lachner, Czech Republic) was used as received.

Poly(5,5-bisbenzimidazole-2,2-diyl-1,3-phenylene) (PBI) was supplied by Hoechst Celanese and used as received as a 10 wt.% *N,N*-dimethylacetamide (DMAc) solution with a lithium chloride content of ~2 wt.%.

Giel *et al. Nanoscale Research Letters* (2017) 12:3

Page 3 of 15

TiO$_2$ powder (rutile modification), dopamine-hydrochloride, and tris(hydroxymethyl)aminomethane (TRIS) buffer (Sigma 7-9™, 99 %) were purchased from Sigma Aldrich, Germany.

Nanotubes Synthesis and Functionalisation

TiNTs were synthesised by hydrothermal treatment. The details of the synthesis method of TiNTs are described elsewhere [30]. A thin PDA layer was created onto the surface of TiNTs by oxidative polymerisation of dopamine-hydrochloride. This procedure involves mixing of 800 ml of TiNT suspension (2 mg/ml) with 1.6 g of dopamine-hydrochloride dissolved in 5 g of TRIS buffer adjusted to pH = 8.5. The PDA coating on TiNTs was carried out for 3.5 h at 25 °C. After coating, the pH was adjusted to 6.4 using 35 wt.% HCl. The suspension was purified using dialysis tubing cellulose membrane and the resulting PDA-functionalised TiNTs (PDA-TiNTs) were isolated using freeze drying.

Preparation of Mixed Matrix Membranes

Two series of MMMs were prepared: PPO-PDA-TiNT MMMs and PBI-PDA-TiNT MMMs. For the preparation of PPO-PDA-TiNT MMMs, PPO was dissolved in chloroform to obtain a 5 wt.% casting solution and stirred for 24 h. The PDA-TiNT was then added to the polymer solution and stirred with a magnetic stirrer for 24 h. The content of PDA-TiNT in the membranes was 1.5, 3, 6, and 9 wt.%, respectively. In case of PBI-PDA-TiNT MMMs, the PBI solution was diluted with DMAc to obtain as well a 5 wt.% polymer solution. The same amounts of PDA-TiNT were added as well to the polymer solutions of PBI. The details of the membrane preparation have been described in the previous work [30]. The resulting membranes had a thickness between 20 and 60 μm.

Characterisation and Measurements

The size and morphology of TiNTs were analysed by using a transmission electron microscope (TEM) Tecnai G Spirit (FEI, 120 kV).

The specific surface area (S_{BET}) of the TiNT and PDA-TiNT samples was measured by a gas adsorption technique on a Gemini VII 2390 (Micromeritics Instruments Corp., Norcross, USA) with nitrogen as the sorbate. The surface area was calculated from the Brunauer-Emmett-Teller (BET) adsorption/desorption isotherm using the Gemini software. It characterises materials in the region of micropores (<2 nm) [41].Calculations were done with a sample density $\rho = 1.3$ g/ml.

The cross section and surface morphology of the membranes were observed using a Quanta 200 FEG scanning electron microscope.

The thermal behaviour of the neat polymers and MMMs were studied on DSC Perkin Elmer 8500. The

heating was performed in two steps. The first step was the continuous heating at 100 °C for 1 h in order to remove the volatiles from the polymer matrix. The second step was the increase of the temperature from 0 to 500 °C at the rate of 100 °C/min in a nitrogen purge (25 cm^3/min).

Wide-angle X-ray scattering (WAXS) experiments were performed using a pinhole camera (modified Molecular Metrology System, Rigaku, Japan) attached to a micro-focused X-ray beam generator (Rigaku MicroMax 003) operating at 50 kV and 0.6 mA (30 W). The camera was equipped with removable and interchangeable Imaging Plate 23 × 25 cm (Fujifilm). Experimental setup covered the momentum transfer (q) range of 0.4–3.6 Å^{-1}. While $q = (4\pi/\lambda)\sin\theta$, where $\lambda = 1.54$ is the wavelength and 2θ is the scattering angle. Calibrations of the centre and sample-to-detector distance were made using Si powder. Samples were measured in transmission mode for 30 min.

The FTIR spectra of membranes were obtained using Spectrum 100 spectrometer (PerkinElmer, USA) equipped with a mercury–cadmium–telluride (MCT) detector in the wavelength range from 650 to 4000 cm^{-1} and universal attenuated total reflectance accessory (ATR) with a diamond prism. Spectral resolution was 4 cm^{-1} with 16 scans taken for each spectrum. The FTIR spectra of the nanotubes (TiNT, PDA-TiNT) and PDA were recorded on a Perkin Elmer Paragon 1000PC FTIR spectrometer using the reflective ATR technique Specac MKII Golden Gate Single Reflection ATR System with a diamond crystal. All spectra were measured in the wavenumber range 450–4400 cm^{-1} with a resolution of 4 cm^{-1} and with 32 scans.

Gas permeability through membranes was determined by the procedure described elsewhere [30]. The permeability P was determined from the increase of pressure Δp_p per time Δt and calculated via the following formula (Eq. 1) [42]:

$$P = \frac{\Delta p_p}{\Delta t} \cdot \frac{V_p \cdot l}{A \cdot p_i} \cdot \frac{1}{RT}, \tag{1}$$

where l is the membrane thickness, A the area, T the temperature, and R the gas constant. Permeabilities are reported in units of Barrer (1 Barrer = 1 × 10^{-10} cm^3(STP) cm/(cm^2 s cm Hg)). The following gases were studied: H$_2$, O$_2$, N$_2$, CH$_4$, and CO$_2$. All gases were used as received from Messer Technogas s.r.o. (Czech Republic) with a purity of 99.99 %. The ideal selectivity $\alpha_{i/j}$ of two gases i and j was determined by the ratio (Eq. 2) [42]:

$$\alpha_{i/j} = P_i/P_j. \tag{2}$$

The accuracy of the measurement is given by the sum of the relative accuracies of each measured term of Eq.

Giel *et al. Nanoscale Research Letters* (2017) 12:3

Page 4 of 15

1. The relative error of $\Delta p_p / \Delta t$ measured with MKS Baratron is smaller than 0.3 % plus the inaccuracy attributed to the resolution of the pressure transducer which is 1/10 of mbar. The relative standard deviation of the calibrated volume is less than 0.1 %, of the membrane area less than 0.5 %, and of the feed pressure 0.2 %. In case of the thickness of the membrane, the value can be measured as precise as 1 μm.

Sorption studies were performed on the gravimetric sorption balance IGA-002, Hiden Isochema, UK, according to the procedure described in [30]. The sorption isotherms were measured by stepwise pressure changes (pressure increase rate 100 mbar/min) within the pressure range of 0.01–4 bar. The sorption balance consists of a large capacity microbalance (5 g) with a resolution of 0.1 μg and excellent long-term stability of ±1 μg.

Results and Discussion

The dried non-modified and modified nanotubes were studied via TEM (Fig. 1). The picture of TiNT (Fig. 1a) demonstrates the formation of long, closed, and almost aggregation-free nanotubes. After modification the nanotubes are completely covered with a thin layer of PDA as it can be seen in Fig. 1b. The obtained nanotubes posses an outer diameter of around 8–12 nm and their length varies from 100 nm to 1 μm. The thickness of the created PDA layer is about 10–12 nm.

From the measurement of the specific surface area, it was found that the S_{BET} of TiNT reduces significantly from 540 to 38 m^2/g through modification with PDA (Table 1). The change in the specific surface area can be attributed to the creation of a thin polymer film on the surface of TiNTs and to the aggregation of the nanotubes.

The structure and chemical interactions of PDA-TiNT were examined by ATR FTIR spectroscopy, in the mid-range between 4000 and 400 cm^{-1}. The IR spectra of nanotubes before and after oxidative polymerisation with PDA are shown in Fig. 2. Based on the literature [43], the broad band in the region of 3660–2350 cm^{-1} can be assigned to O–H stretching vibrations indicating the presence of hydroxyl groups on the nanotube surface. This region also corresponds to vibrations of adsorbed water molecules what confirms the small peak at around 1636 cm^{-1} (H–O–H bending vibrations). The IR spectrum of TiNT exhibits a band located at around 922 cm^{-1} which might be attributed to the Ti–O stretching vibrations involving non-bridging oxygen. The broad region around 800–400 cm^{-1} corresponds to the Ti–O–Ti vibrations in the nanotube skeleton.

In the IR spectrum of aromatic PDA a broad region between 3680 and 2350 cm^{-1} can be distinguished which can be ascribed to N–H stretching (3500–3200 cm^{-1}), C–H stretching (3100–3000 cm^{-1}), and H-bonded O–H stretching (3570–3200 cm^{-1}). Moreover, the absorption peaks in the 1650–1430 cm^{-1} range correspond to C=C stretching in the benzene ring; however, they are partially overlapped with the ring stretching region of heterocycles containing N–H groups (1600–1300 cm^{-1}). Similarly, the C–N stretching bands of aromatic amines appear in the region 1360–1250 cm^{-1} and overlap the peak attributed to the O–H bending in phenols (1410–1310 cm^{-1}). The peak at 1052 cm^{-1} might correspond to the in-plane C–H bending in aromatic ring [43, 44].

The functionalisation of titanium nanotubes by PDA polymer led to visible changes in IR spectra what might be due to H-bonding interactions between both components (Fig. 2). As a first confirmation, we can point out the broadening of the band in 3680–1810 cm^{-1} region. Accordingly, in the region of lower wavelengths new peaks occur (1628, 1038 cm^{-1}) and some peaks become narrower and shifted to higher wavelengths (e.g. 1552, 1294 cm^{-1}) compared to the spectra of PDA. It is assumed that those changes are a result of hydrogen bond interactions between N–H and O–H groups of the PDA
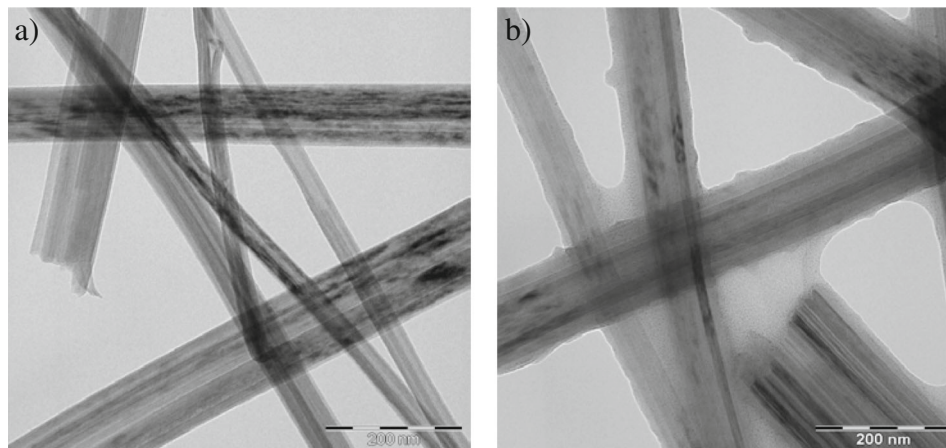

Fig. 1 TEM images of TiNTs (**a**) and PDA-TiNTs (**b**)

Giel *et al. Nanoscale Research Letters* (2017) 12:3

Page 5 of 15

**Table 1** Results of S_{BET} determination

Sample	S_{BET} (m^2/g)
TiNT	540.2
PDA-TiNT	38.4

polymer and the Ti-O groups of the nanotubes. Nevertheless, the exact interpretation of the peaks is not possible due to measurement difficulties.

The incorporation of PDA-TiNTs into the PBI matrix caused broadening of the peak in the region between 3680–2350 cm^{-1} (Fig. 3a). The width of the peak at 1609 cm^{-1}, corresponding to C=N stretching, changed also slightly. The process was more intensive for samples with higher content of nanotubes and might signify the H-bonding interactions between N–H, O–H, Ti–O, and C=N groups present in the system.

In the case of PPO-PDA-TiNT *MMMs* (Fig. 3b) no changes of any peak has been observed, although PDA possess –OH groups which are suitable to interact with the oxygen atom present in PPO. However, the aromatic rings of PDA are very bulky, wherefore it is assumed that the interactions between the PDA-TiNT and PPO are restricted because of steric hindrance.

The influence of nanotubes on the polymer matrix was studied by WAXS. Figure 4 shows the WAXS pattern for modified nanotubes, PBI, and PBI-PDA-TiNT MMM with a loading of 6 wt.% of PDA-TiNTs. As can be seen from Fig. 4, the WAXS pattern obtained from PDA-TiNT illustrates two amorphous peaks at 2 = 8° and 18°, respectively, and three crystalline peaks at 2 = 27°, 36°, and 41°. In case of pure PBI, two broad amorphous peaks were detected at 2 = 20° and 25°. With the addition of PDA-TiNT into PBI matrix, the PBI-PDA-TiNT MMM still remains its amorphous structure. Besides, some additional crystalline peaks could be detected,
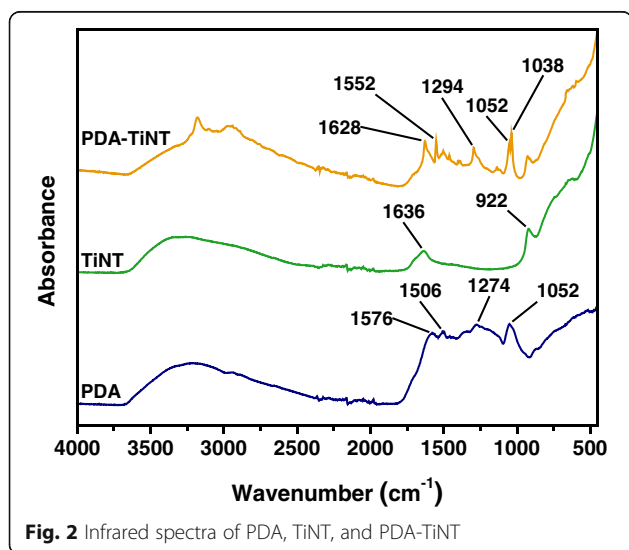
which can be assigned to PDA-TiNTs present in the PBI matrix.

DSC analysis was used to measure the T_g of PBI-PDA-TiNT and PPO-PDA-TiNT MMMs. This method has been applied in several studies to investigate the influence of fillers in nanocomposites on the T_g. Changes in T_g were mostly ascribed to changes in chain mobility [9, 20], but effective links between the polymeric chains and the nanotube surface might be as well of relevance [6, 10]. Table 2 *depicts* the values of T_g of PBI-PDA-TiNT MMMs and PPO-PDA-TiNT MMMs, respectively, obtained from DSC measurements.

The T_g for PBI was found to be 413.5 °C which is similar to published data [45].With addition of 6 wt% of PDA-TiNT the T_g noticeably increased. It is assumed, that the aromatic rings of PDA, which are attached on the surface of TiNT, reduces the segmental mobility of PBI polymer chains. In addition, the PDA-TiNTs seem to be able to interact with neat PBI as FTIR studies showed.

PPO-PDA-TiNT MMMs were characterised by no significant change in T_g compared to neat PPO. It is assumed that the slight differences arouse from changes in chain mobility, but not from interaction between the functional groups of PDA-TiNT with PPO which is in accordance with the FTIR results.

For fabricating MMMs, the fillers should disperse well in the polymer matrix. Therefore, TiNT was functionalised with PDA in order to enhance the TiNT dispergation and adhesion with the polymer matrix. The distribution of PDA-TiNT in the polymer matrix was studied by SEM. Figure 5 presents the SEM morphology of the cross section and surface of neat PBI and PPO (Fig. 5a, b; e, f), respectively, as well of PBI-PDA-TiNT and PPO-PDA-TiNT with 6 wt.% of PDA-TiNT (Fig. 5c, d; g, h). It was observed that the membranes are without undesired cracks or pin-holes. When PDA-TiNTs were incorporated into PPO, the resulting MMMs exhibited rougher surface in comparison to the neat polymer and PBI-PDA-TiNT MMMs, respectively. As the surface micrographs of the MMMs depicts, the functionalised PDA-TiNTs tend to disperse quite well in the PBI and PPO matrix independently on the PDA-TiNT content. However, it seems that the nanotubes form agglomerates, as can be seen on the surface and in the cross section of both MMMs, which might arise from intermolecular forces and physical entanglements between the modified TiNTs. Nevertheless, it seems that the nanotubes have a good adhesion to the polymer matrix, because there is no evidence of interfacial voids in the prepared MMMs. Also, the results of the permeability measurements suggest the absence of interfacial voids as described later in this paper.

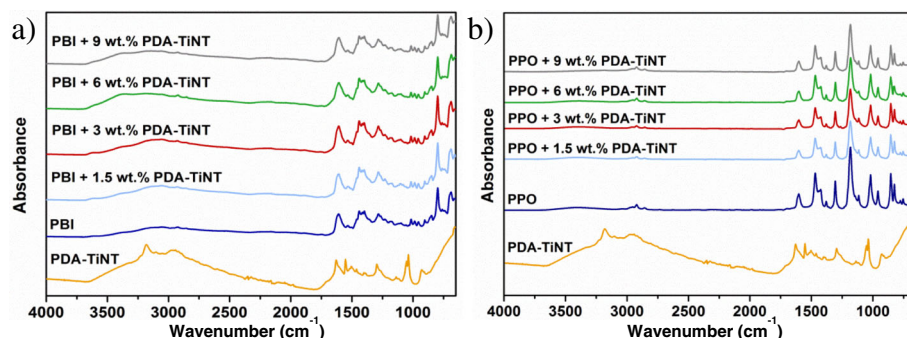Determination of gas permeability is a useful method for evaluating membrane performance and can also

Fig. 2 Infrared spectra of PDA, TiNT, and PDA-TiNT

Giel *et al. Nanoscale Research Letters* (2017) 12:3

Page 6 of 15

Fig. 3 Infrared spectra of PDA-TiNT (**a**, **b**), PBI, and PBI-PDA-TiNT MMMs (**a**) as well as PPO and PPO-PDA-TiNT MMMs (**b**) with various amount of TiNT

provide the information about the filler-polymer matrix compatibility. Gas separation performance of a membrane can be determined by the membrane permeability (Fig. 6a, b) and selectivity (Fig. 6c, d). In this study, both types of MMMs were tested for five different gases in order to investigate the effect of PDA-TiNT on membrane separation performance. Figure 6a, b shows the gas permeability coefficients of the PBI-PDA-TiNT MMMs (Fig. 6a) and PPO-PDA-TiNT MMMs (Fig. 6b) as a function of PDA-TiNT weight concentration. In general, for all membranes, permeability coefficients decreased in the order $H_2 > CO_2 > O_2 > N_2 > CH_4$ indicating that the separation mechanism is based on solution-diffusion mechanism which is typical for most glassy polymers [46]. With increasing amount of nanotubes in PBI-PDA-TiNT MMMs and PPO-PDA-TiNT MMMs, respectively, permeability coefficients tend to decrease.

Dependent on the material used, separation properties are different. As anticipated, PBI is less permeable than PPO, because of its rigid aromatic molecular structure and its relatively high chain packing density [15, 31]. High permeability of PPO among aromatic polymeric

membranes can be attributed to the ether linkages, which introduce more flexibility to the polymer chain, steric hindrance of the methyl groups and lower packing density due to the absence of polar groups [47, 48].

In both matrices, the presence of filler causes a decrease in permeability. With the increase of the PDA-TiNT amount the permeability drops. As generally known, the presence of fillers brings a sort of physical barriers in the membrane that act as obstacles in the diffusive path of a gas molecule permeating across the membrane. These obstacles increase the tortuosity for gas molecules in the present MMMs, thus decrease its permeability [5, 34].

Besides, the orientation of nanotubes inside the matrix plays also a role in the separation characteristic. It was reported in the literature that MMMs with well oriented, open-ended CNTs, which are accessible for gas molecules, exhibit increased permeability [23, 25, 49]. In the present study, as SEM results show, PDA-TiNTs are randomly orientated, sometimes interconnected or even agglomerated. Therefore, it is concluded that the accessibility of the tunnels for gas molecules is limited, and PDA-TiNTs act more as a barrier which results in permeability decrease.

Another important aspect is the influence of modifier on the membrane performance. From the obtained permeability and SEM analysis, it can be concluded that both polymers adhere well to PDA-TiNTs, although FTIR studies could detect only changes in the FTIR spectra of PBI upon addition of PDA-TiNTs. Therefore, we can conclude that the sufficient adhesion between PPO and PDA-TiNT might be caused by van der Waals
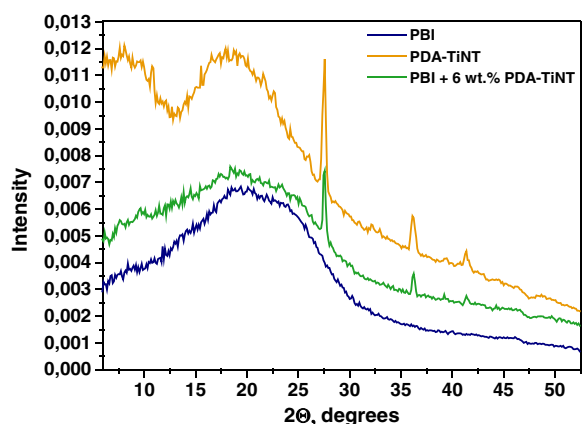

Fig. 4 WAXS diffractogram of PDA-TiNT, PBI, and PBI with 6 wt.% of PDA-TiNT

Table 2 T_g of neat polymers and MMMs

Sample	Amount of PDA-TiNT in membrane	T_g (°C)
PBI	0 wt.%	413.5
PBI-PDA-TiNT	6 wt.%	424.6
PPO	0 wt.%	214.6
PPO-PDA-TiNT	6 wt.%	214.4

Giel *et al. Nanoscale Research Letters* (2017) 12:3
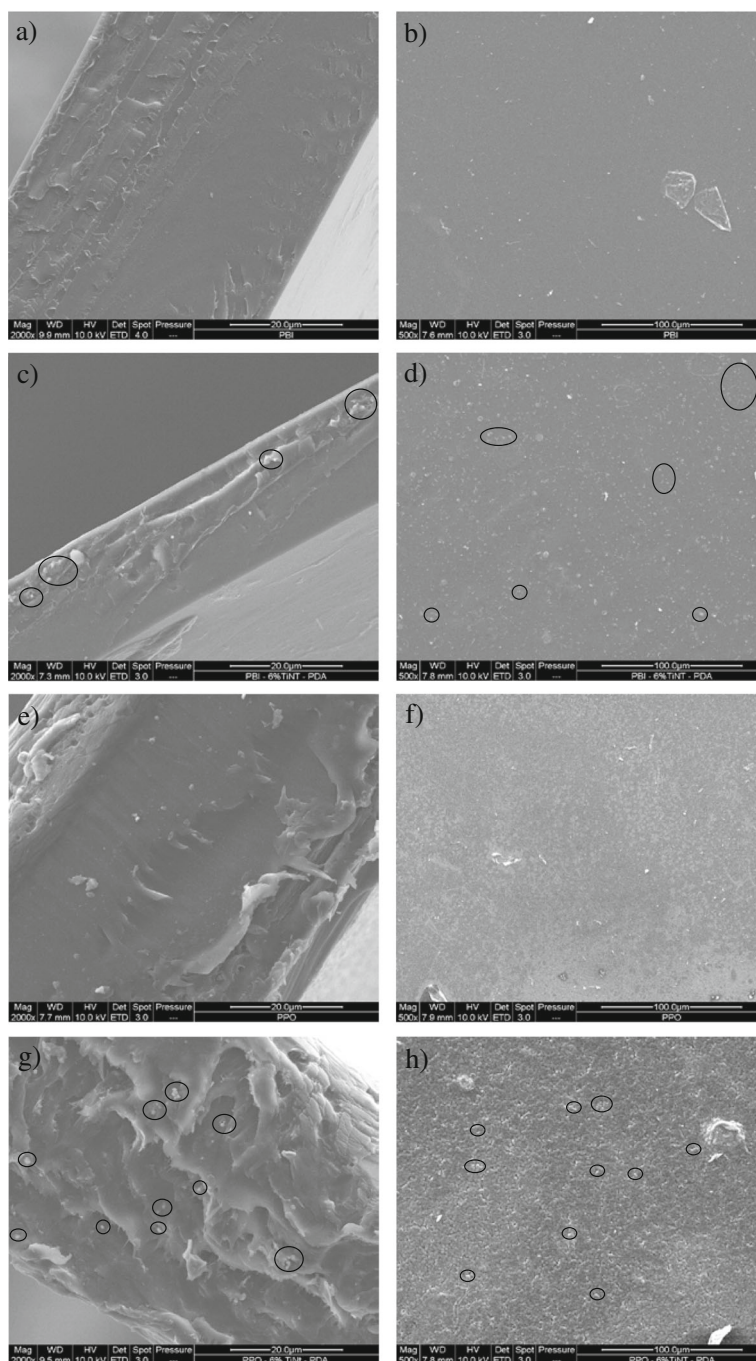
Page 7 of 15

Fig. 5 Cross sections and surface image of PBI (**a**, **b**), PBI-PDA-TiNT 6 wt.% (**c**, **d**), PPO (**e**, **f**), and PPO-PDA-TiNT 6 wt.% (**g**, **h**)

forces [50]. In case of weaker interactions, gas accessible voids would be formed at the interface of PDA-TiNT and PPO, which in turn would result in a major boost of gas permeability, whereas selectivity would remain the same or would be close to the one of neat polymer [8, 51, 52].

Even though modifications led to improved adhesion for both polymers, it is interesting to note that permeability and selectivity values of PBI-PDA-TiNT MMMs are lower in comparison to those of PBI membranes with non-modified TiNTs. This result suggests that the gas transport properties of PDA have to be taken into account. When one compares the results of PPO-TiNT MMMs from earlier work [30] with the results of this study, a decrease in permeability can be observed for the PPO-PDA-TiNT MMMs along with an
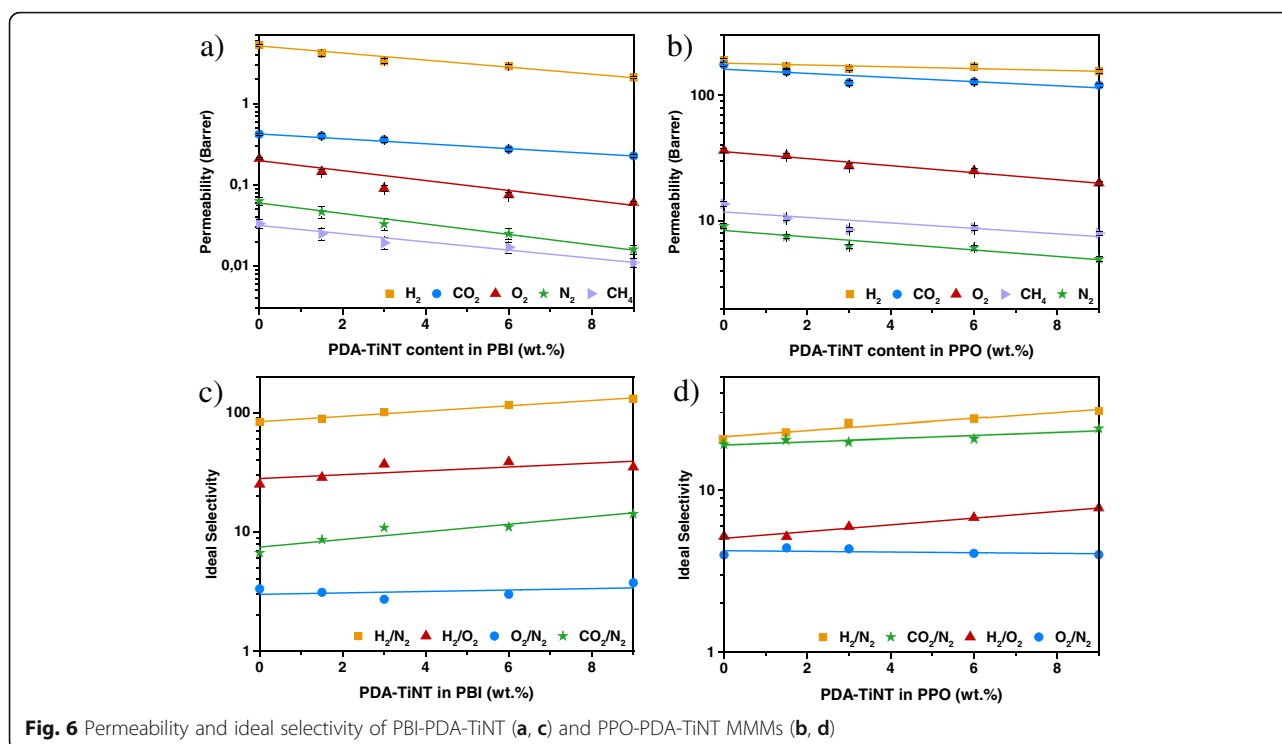
Giel *et al. Nanoscale Research Letters* (2017) 12:3

Page 8 of 15

Fig. 6 Permeability and ideal selectivity of PBI-PDA-TiNT (**a**, **c**) and PPO-PDA-TiNT MMMs (**b**, **d**)

increase in selectivity. In contrary, PPO-TiNT MMMs showed an increase in permeability while selectivity remained almost constant. The observed increase can be explained by formed voids between the non-modified TiNTs and the PPO, which have negligible resistance to the flow of gas and thus cause an increase in permeability. The voids, however, are poorly selective, wherefore the selectivity remains constant. Thus, functionalisation of TiNTs improves the adhesion between the two phases and consequently minimise undesirable voids, which results in a decline in permeability.

The dependence of ideal selectivity of selected gas pairs on the concentration of PDA-TiNT in PBI (Fig. 6c) and PPO (Fig. 6d), respectively, is presented in Fig. 6. As the plots indicate PDA-TiNTs influence mainly the gas selectivity of PBI based MMMs. Addition of 9 wt.% PDA-TiNT to PBI resulted in an increase of 112 and 63 % in the selectivity of CO_2/N_2 or CO_2/CH_4, respectively. Similarly, the selectivity of H_2/N_2, H_2/O_2, and O_2/N_2 increased by 57, 40, and 12.50 %, respectively. The high selectivity values for CO_2/N_2 and CO_2/CH_4 can be explained by the polar functional groups of PDA on the TiNTs, confirmed by FTIR. Those polar groups usually exhibit a stronger interaction with polar gases, such as CO_2, than with nonpolar gases, e.g. N_2 or CH_4. Thus, the polar gas solubility can be enhanced and the gas permeability can be increased which facilitates the improvement of the total CO_2/N_2 or CO_2/CH_4 selectivity [12]. Ideal selectivities of the other gas

pairs further demonstrate that gases with a smaller kinetic diameter, e.g. H_2 permeate easily through the intimately connected PBI matrix with PDA-TiNT than bigger gas molecules, e.g. N_2 or O_2, resulting in higher selectivity ratio.

As for PPO-PDA-TiNT MMMs, gas selectivities increase for all gas pairs besides O_2/N_2, which remains nearly constant, meaning that the permeabilities of O_2 and N_2 decreased at the same rate. Analogically, selectivity increase for the gas pairs H_2/N_2 and H_2/O_2 are similar (50 %; 49 %). The CO_2 over N_2 selectivity enhancement (25 %) was larger than over CH_4 (17 %), even though the kinetic diameter of CH_4 (3.8 Å) is greater than the one of N_2 (3.64 Å). However, CH_4 solubilise better in PPO than N_2, wherefore CH_4 preferably permeates through the MMM than N_2, which is in accordance with the literature [53–55].

Comparing the results of PBI-PDA-TiNT and PPO-PDA-TiNT MMMs, one can see that the addition of PDA-TiNT influence the separation performance of PBI-PDA-TiNT MMMs more significant than of PPO-PDA-TiNT MMMs.

The differences in permeabilities of each MMMs can be better understood by analysing the diffusion and solubility coefficients, since the permeability P of a gas is proportional to the diffusivity D and solubility S of a gas in the membrane ($P = D \times S$) [42]. Moreover, for a given polymeric membrane, D mainly depends on the kinetic diameter of a gas molecule and S mainly on the

Giel *et al. Nanoscale Research Letters* (2017) 12:3

Page 9 of 15

condensability of a gas molecule [20]. Upon adding inorganic nanofillers, gas transport properties may be affected in the following ways: (a) the incorporation of nonporous or impermeable fillers in a polymer membrane will lead to a reduction of permeability due to increased tortuosity of the diffusion path as well as reduced solubility of the separating gas molecules in the polymer matrix [34], (b) the interactions between the nanoparticles and the polymer chains or penetrants, respectively, are strong and significantly change the diffusivity and solubility of penetrants [25], (c) the nanoparticles affects the polymer chain stiffness or mobility and therefore the gas diffusion by increasing or decreasing of the free volume of the polymer chains [34], (d) the interaction between polymer-chain segments and nanoparticles may increase or decrease the formation of voids (defects between polymer/nanoparticle interface), and therefore deteriorates the gas diffusion [56], (e) the modification of nanoparticles introduces functional groups on the surface of the nanoparticles, which may interact with more condensable gases such as CO_2 and therefore improve the gas' solubility in the MMMs [57]. Figure 7 shows the diffusion and solubility coefficients with the respective selectivities of neat PBI and PBI-PDA-TiNT MMMs. The values for neat PPO and PPO-PDA-TiNT MMMs are presented in Fig. 8.

As can be seen from Figs. 7a and 8a, gas diffusivities of all studied gases decreased with PDA-TiNT loading. After incorporation of 9 wt.% PDA-TiNTs to PBI,

diffusion coefficients for H_2, O_2, N_2, CO_2, and CH_4 decreased by around 37, 32, 28, 46, and 39 %, respectively (Fig. 7c). In case of PPO, the diffusion coefficients decreased about 54, 38, 46, 52, and 48 % for H_2, O_2, N_2, CO_2, and CH_4, respectively (Fig. 8c). These results suggest that there are no voids between PDA-TiNTs and polymer chains leading to higher gas diffusion resistance and therefore to decreased diffusion coefficients. If there had been some voids, gas separation performance would be affected to a great extent, because the gaps at the interface between the nanotubes and the polymer provide a less resistive route for gases; thus, gas permeability would increase. Moreover, it is assumed that the addition of PDA-TiNTs facilitates polymer chain packing and reduces the free volume between the polymer chains due to the decreased diffusion coefficients. In addition, it seems, that the channels of the added nanotubes are not readily accessible for the gas molecules, elsewise the prepared MMMs would possess higher gas permeabilities due to a more effectively transport of the gas molecules through the tunnels of the nanotubes.

Despite the decrease in diffusivity, the solubility of PBI-PDA-TiNT MMMs remained relatively unchanged for H_2, N_2, O_2, and CH_4 with the increase of nanotubes, besides for CO_2 (Fig. 7b). CO_2 is a more condensable gas than all the other studied gases. The increased gas condensability leads to the enhancement of the solubility of the gas in the polymer matrix, which confirms the dominancy of the solution mechanism in the permeation
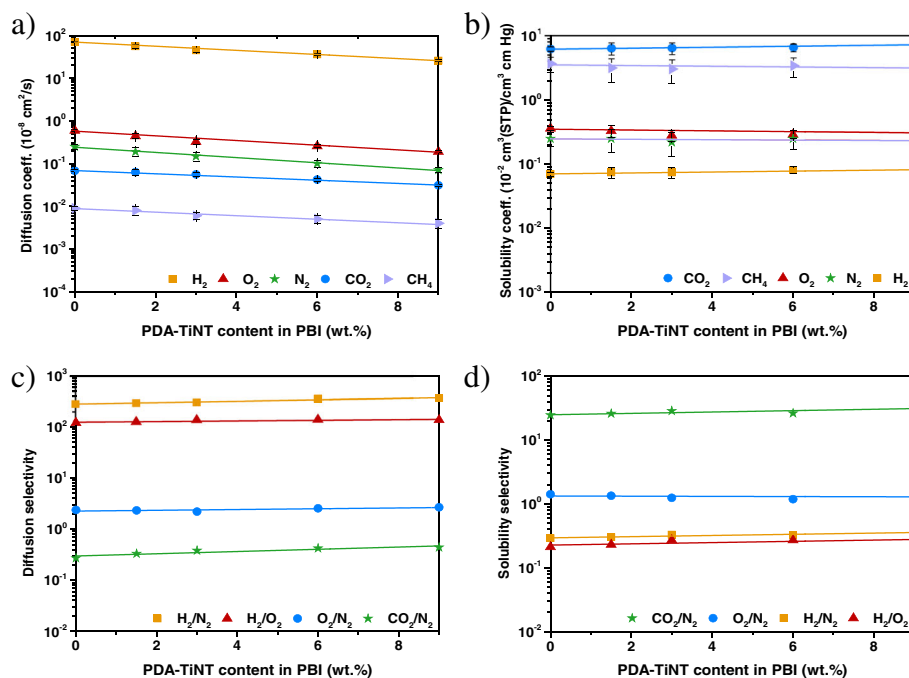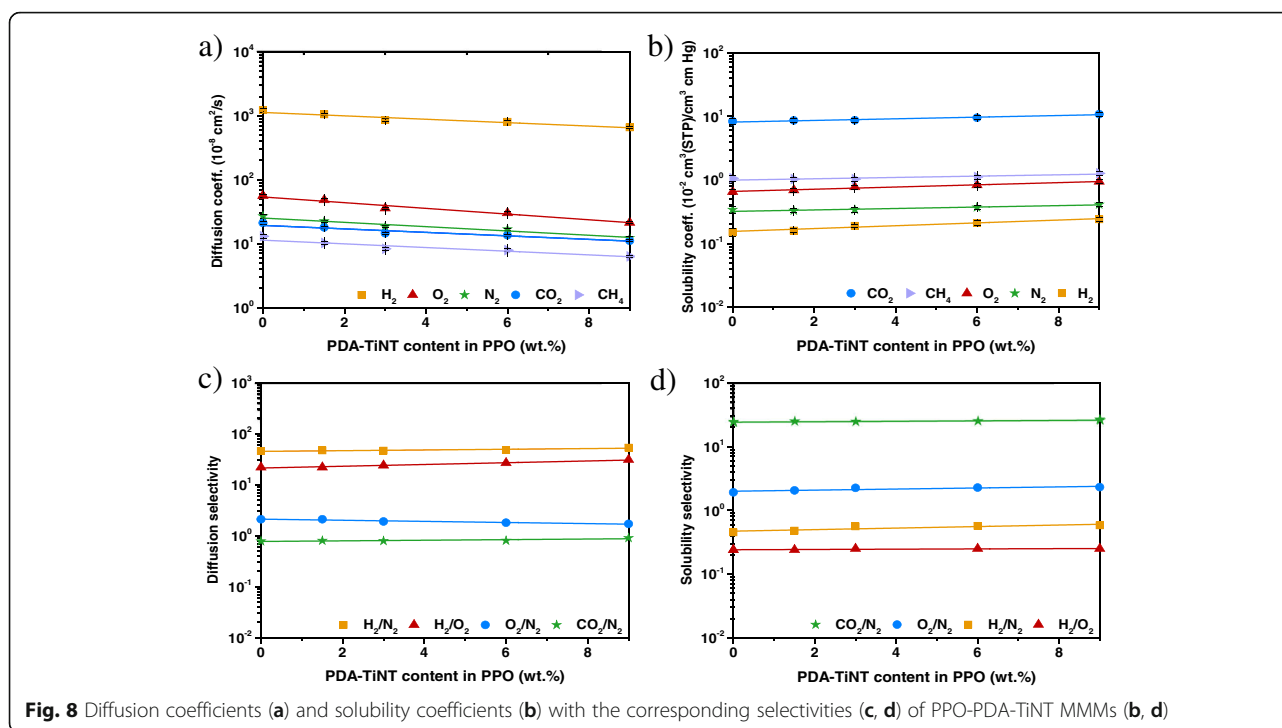

Fig. 7 Diffusion coefficients (**a**) and solubility coefficients (**b**) with the corresponding selectivities (**c**, **d**) of PBI-PDA-TiNT MMMs (**b**, **d**)

Giel *et al. Nanoscale Research Letters* (2017) 12:3

Page 10 of 15

Fig. 8 Diffusion coefficients (**a**) and solubility coefficients (**b**) with the corresponding selectivities (**c**, **d**) of PPO-PDA-TiNT MMMs (**b**, **d**)

of CO_2 through the MMMs upon addition of PDA-TiNTs. Moreover, the strong polar affinity between the functional groups of PDA on the surface of the nanotubes and CO_2 results in an increased CO_2 solubility. With the increase of PDA-TiNT in the matrix the CO_2 solubility increases due to the larger content of CO_2-facilitated transport sites in the membranes, which leads to a steady increase of CO_2/N_2 solubility selectivity (Fig. 7d). In contrary, the solubility values of the PPO-PDA-TiNT MMMs showed for all gases an increase in solubility coefficients (Fig. 8b). Highest increase of solubility selectivity was found for the gas pair H_2/N_2, which might be due to the differences in kinetic diameters of these gas molecules. If one compares the solubility values of the neat polymers, it can be found that the solubility coefficients (Fig. 8d) of all gases besides CH_4 are higher for PPO than for PBI (Fig. 7d); thus, the gases can solubilise better in PPO than in PBI. The differences in the solubilities between those two polymers are caused by the different molecular structures of PBI and PPO.

From the obtained diffusivity and solubility results (Figs. 7, and 8), it can be concluded that the addition of PDA-modified TiNTs to PBI or PPO deteriorates the permeability properties by decreasing gas diffusivity of all studied gases due to enhanced chain packing density and reduced chain segment mobility. In addition, the incorporation of modified nanotubes into PBI or PPO enhances the solubility of condensable gases by increasing the number of functional groups. Moreover, it is believed that the modified TiNTs act as impermeable filler which

are lowering the permeability of all gases; hence, hindering the diffusion of the gases through the MMMs. Furthermore, the MMMs have no evidence of unselective voids.

To clearly display the membrane performances, some of the pure gas data have been encompassed in the Robeson plot (Fig. 9). This plot represents the limits of the selectivity-permeability behaviour of neat polymers via the upper bound [14, 58]. Well above the upper bound is the commercially attractive region for membrane preparation [52]. Most inorganic membranes are situated there. However, these materials are expensive and difficult to prepare, wherefore the combination of polymers with fillers seems to be a promising solution to exceed this upper bound [8]. Figure 9 *depicts* the existing literature data of selected MMMs based on nanotubes [12, 20–25, 30] and the data of selected membranes of the present work in order show the impact of nanotubes on different types of polymers and to show the upper bound limits for the gas pairs H_2/N_2, CO_2/CH_4, O_2/N_2, and CO_2/N_2.

As can be seen from Fig. 9 the composition of MMMs plays an important role. Depending on the choice of material and filler, the obtained results fall close to the trade-off line. The addition of different types of nanotubes caused either an increase in permeability and decrease in selectivity or vice versa. Only in the case of Matrimid-based MMMs, an increase in both parameters could be observed. Nevertheless, additional studies on MMMs need to be performed in order to overcome this upper bound.

Fig. 9 Robeson diagrams of the gas pairs: **a** H_2/N_2, **b** CO_2/CH_4, **c** O_2/N_2, and **d** CO_2/N_2
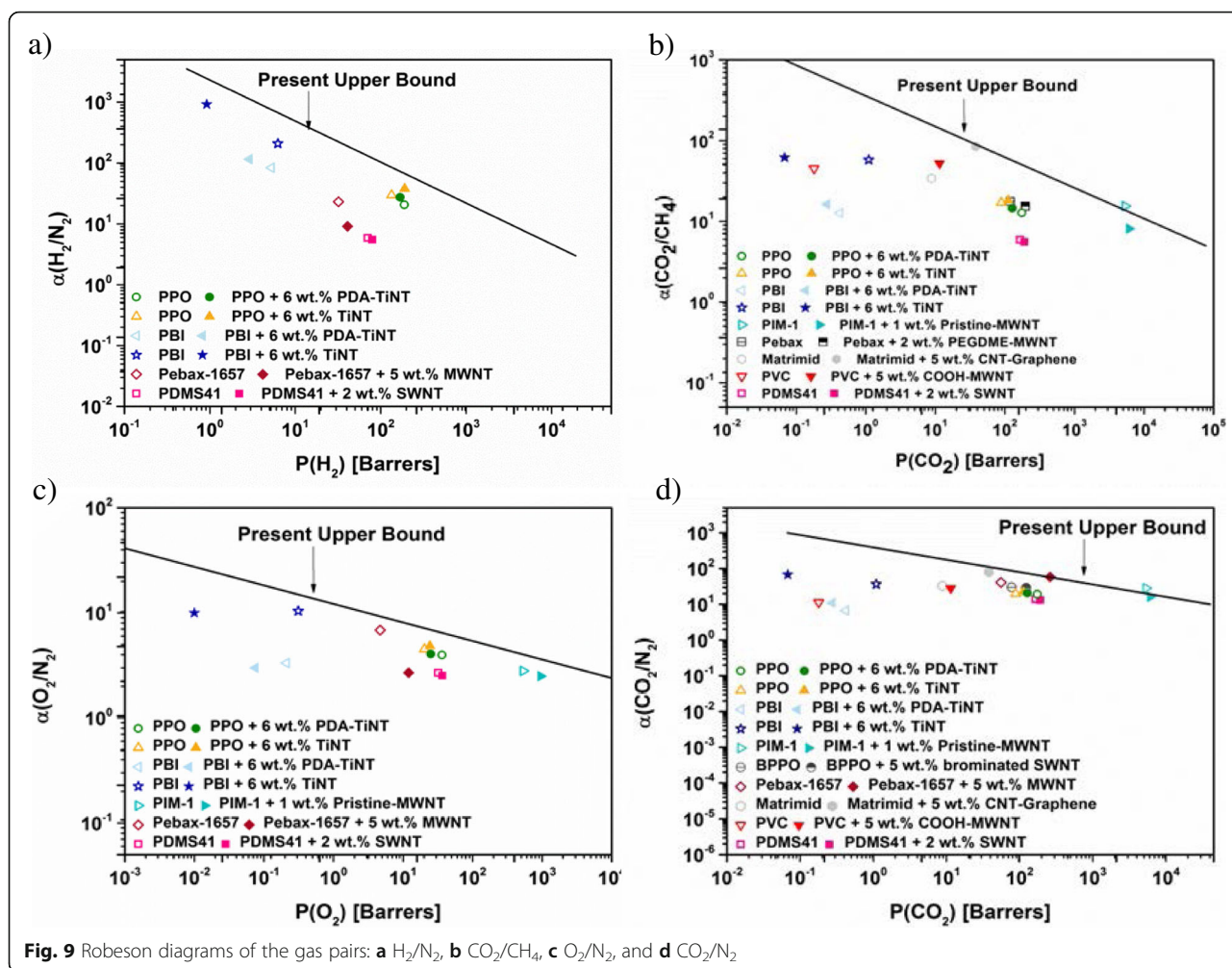
Table 3 presents additionally the permeability and selectivity data of various types of PPO and PBI MMMs prepared in this work [30–34] and the ones reported elsewhere.

Table 3 reveals that PPO and PBI have been utilised in several types of research as a polymer matrix for membrane preparation. The gas transport properties of the neat membranes are in accordance with those of other works. Upon addition of any kind of filler, different effects on the separation performance can be observed. In general, the addition of silica, ZIF-8, SBA-15, and non-modified or modified TiNTs, respectively, to PPO or PBI cause an increase in gas selectivities. As far as permeabilities are concerned, they either increased or decreased. This can be explained by good adhesion of the polymer chains on the surface of the filler. Poor adhesion of the polymer onto the filler can cause voids between the interface of polymer chains and fillers, which leads to an increase in permeability, whereas selectivity remains almost the same. In conclusion, the employment of

fillers can result in high selective membranes with superb permeation rates depending on the choice of polymer and filler.

Figure 10 presents the sorption isotherms of neat PBI membrane and 6 wt.% PBI-PDA-TiNT MMM, respectively, for the gases H_2, O_2, N_2, CH_4, and CO_2.

For describing the sorption behaviour of glassy polymers, the so-called dual-mode sorption model is often used (Eq. 3) [46, 59–61].

$$C = k_D p \; + \; \underbrace{\frac{C_H' b p}{1 + b p}}_{\text{Langmuir term}},$$
$$\underbrace{}_{\substack{\text{Henry's}\\\text{law term}}}$$

(3)

where C is the total gas concentration in a glassy polymer, k_D is the Henry's law parameter, C_H' is the Langmuir sorption capacity, and b is the Langmuir affinity parameter.

Table 3 Technical achievable performance according to types of membranes investigated by different research groups

Polymer	Filler (wt.%)	Permeability (Barrer)					Selectivity				Reference
		P_{H2}	P_{O2}	P_{N2}	P_{CH4}	P_{CO2}	$a_{CO2/N2}$	$a_{CO2/CH4}$	$a_{H2/N2}$	$a_{H2/CO2}$	
PPO	SBA-15[a]										[32]
	0	134.05	–	3.80	4.70	69.20	17.9	14.8	37.1	2.1	
	10	92.82	–	2.10	1.51	53.20	26.8	36.0	49.7	1.8	
	Silica[a]										[33]
	0	82.17	–	–	–	48.81	–	–	–	1.68	
	10	548.7	–	–	–	154.05	–	–	–	3.56	
	TINT[a]										[30]
	0	134.255	20.326	4.508	5.203	88.7	19.68	17.05	29.78	1.51	
	6	190.532	24.379	5.035	6.135	112.298	22.3	18.3	37.84	1.7	
	TINT[b]										This work
	0	188.88	36.41	9.14	13.716	175.04	19.15	12.76	20.66	1.08	
	6	168.68	25.00	6.14	8.8	127.78	20.81	14.52	27.48	6.75	
PBI	ZIF-8[a]										[31]
	0	4.1	–	–	–	0.46	–	–	–	8.9	
	30	82.5	–	–	–	6.9	–	–	–	12.0	
	Silica[a]										[34]
	0	–	–	0.007	0.005	0.025	3.5	4.96	–	–	
	20	–	–	0.002	0.010	0.11	71.3	11.4	–	–	
	TINT[a]										[30]
	0	6.268	0.312	0.030	0.019	1.101	36.7	57.95	208.93	5.693	
	6	0.920	0.010	0.001	0.001	0.068	68	68	920	13.53	
	TINT[b]										This work
	0	5.24	0.21	0.063	0.033	0.421	6.68	12.64	83.17	12.45	
	6 wt.%	2.90	0.075	0.025	0.017	0.275	11.00	16.18	116	10.55	

[a]Non-modified
[b]Modified

At low to moderate pressures, the sorption is determined by the Langmuir term and describes the non-equilibrium region of the curve. Furthermore, it characterises the sorption on the holes or "microvoids" from the non-equilibrium nature of glassy polymers. At higher pressures, Henry's law solubility predominates. Its corresponding Henry's law term describes the equilibrium region and is related to the dissolution of gases into the dense equilibrium structure of rubbery polymers.

In general, the measured sorption data for the more condensable gases CO_2 and CH_4 can be well fitted by the dual-mode sorption model (Fig. 10). Even the lower condensable gases N_2 and O_2 exhibit slightly nonlinear pressure dependence. In case of H_2, which does not

Fig. 10 Sorption isotherms of PBI (**a**) and 6 wt.% PBI-PDA-TiNT MMM (**b**)

Giel *et al. Nanoscale Research Letters* (2017) 12:3
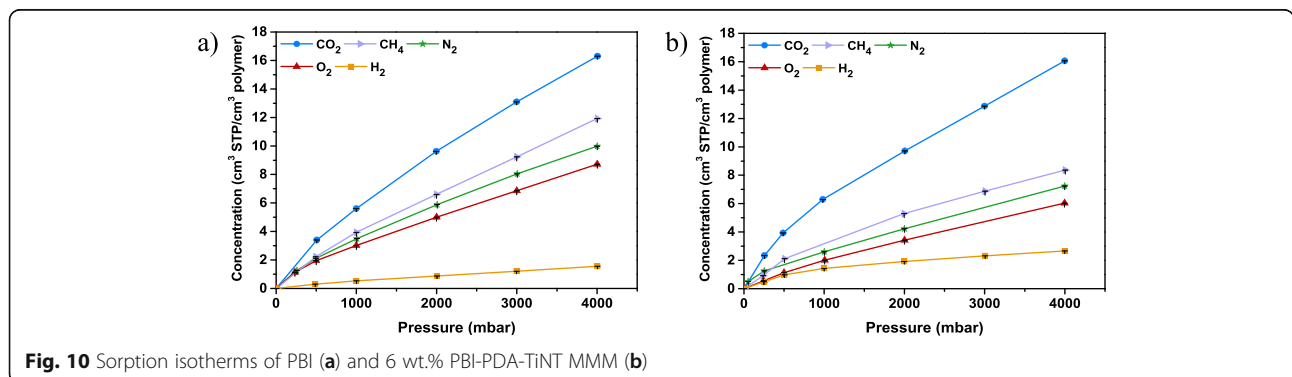
Page 13 of 15

exhibit significant gas sorption, follows the Henry's type gas sorption model, which demonstrates a linear relationship of gas sorption with pressure.

For PBI, sorption isotherms are similar to previously reported ones [30]. In contrary, the 6 wt.% PBI-PDA-TiNT MMM (Fig. 10) exhibits a significant decrease in gas sorption capacity of CH_4, N_2, O_2, and H_2. In previous study with non-modified TiNTs, it was found that the addition of fillers increase the sorption capacity [30], which is in agreement with other published data of MMMs made of nanotubes or other nanoparticles, respectively [56, 62, 63]. In the present case, functionalisation of TiNTs alters the lattice structure of TiNTs which led to a remarkable decrease in the specific area as the values of Table 1 show. This might cause a decline in the sorption capacity of the surface or inner side of TiNTs. Besides, functionalisation improves the filler-polymer interface compatibility for MMMs as can be concluded from IR results, wherefore the gas molecules cannot adsorb in the interlayer spacing between polymer and nanotubes. These major changes achieved in the material's structure lower considerably its sorption capacity for the gases CH_4, N_2, O_2, and H_2.

In case of CO_2, the sorption capacity of the 6 wt.% PBI-PDA-TiNT MMM is in the same amount as of neat PBI membrane due to the inclusion of new sorption sites throughout the addition of modified nanotubes. The abundant CO_2 selective groups, on the surface of TiNTs, enlarge the CO_2 adsorption capacity due to increased polar interactions between the gas molecules and the existing functionalised surface. Similar trends of increased CO_2 sorption capacity were also observed in other reported MMMs [12, 63] and were demonstrated in our previous study with non-modified TiNTs [30]. To conclude, the improvement of sorption capacity by PDA-TiNTs can be attributed to the increase of sorption sites.

Conclusions

MMMs were prepared using TiNTs functionalised with PDA and a PBI and PPO, respectively, as the polymer matrix. TEM and S_{BET} analysis have confirmed the successful PDA functionalisation of TiNTs. The SEM images of the prepared MMM revealed that the functionalised TiNTs are well dispersed throughout the both matrices. Besides, it seems that the nanotubes form agglomerates in the membrane due to functionalisation by PDA. As DSC studies showed, with addition of 6 wt% of PDA-TiNT to PBI the T_g noticeably increased, whereas for the PPO matrix not. According to FTIR studies, PBI and PDA-TiNT interacts possibly via hydrogen bonds. In contrary, no interactions between PPO and PDA-TiNT were observed. In any case, it seems, there is good interfacial adhesion and the absence of voids between PDA-TiNTs and both polymer matrices, as the gas

permeabilities decreased for all gases with the addition of PDA-TiNTs. Lowest permeabilities were observed with the highest content of PDA-TiNT in the MMMs. It is clear that addition of SWNTs to a polymer matrix can improve certain selectivities as well as permeabilities of small molecules. On the other hand, the addition of TiNTs to a polymer matrix can improve certain gas selectivities, especially for CO_2/N_2 and CO_2/CH_4. Further, the sorption capacity of neat PBI and PBI-PDA-TiNT was studied for H_2, O_2, N_2, CH_4, and CO_2. The sorption isotherms elucidated that the presence of PDA-TiNTs in PBI has a positive effect on CO_2 sorption.

Abbreviations
ATR: Attenuated total reflectance; BET: Brunauer-Emmett-Teller; CNT: Carbon nanotube; MCT: Mercury–cadmium–telluride; MMM: Mixed matrix membrane; MOF: Metal organic framework; MWNT: Multi-walled nanotubes; PBI: Poly(5,5-bisbenzimidazole-2,2-diyl-1,3-phenylene); PDA: Polydopamine; PDA-TiNT: PDA-functionalised TiNT; PPO: Poly(2,6-dimethyl-1,4-phenylene oxide); S_{BET}: Specific surface area; TEM: Transmission electron microscope; TiNT: Titanate nanotube; WAXS: Wide-angle X-ray scattering

Symbols
A: Membrane area; b: Langmuir affinity constant; C: Total gas concentration; c_H: Langmuir capacity constant; k_D: Henry's constant; l: Membrane thickness; P: Permeability; p: Penetrant partial pressure; p_i: Feed pressure; p_p: Pressure increase; R: Ideal gas constant; S: Solubility coefficient; T: Temperature; t: Time; V_p: Volume of the product part

Greek Symbol
a: Selectivity

Authors' Contributions
The concept and the design of the study were carried out by VG. VG prepared the membranes and studied the gas permeation and sorption properties. JK fabricated the nanotubes and performed the measurements on DSC. MP carried out the studies on FTIR. VG, MP, and JK collaborated in the acquisition, analysis, and interpretation of the data as well as in writing and reviewing the manuscript. ZP revised the manuscript critically for important intellectual content. All authors read and approved the final manuscript.

Competing Interests
The authors declare that they have no competing interests.

References
1. Van der Bruggen B (2012) The separation power of nanotubes in membranes: a review. ISRN Nanotechnol 2012:1–17. doi:10.5402/2012/693485
2. Boudon J, Papa A, Paris J, Millot N (2014) Titanate nanotubes as a versatile platform for nanomedicine. In: Seifalian A, De Mel A, Kalaskar DM, editors. Nanomedicine. One Central Press, pp 403–428
3. Ahn CH, Baek Y, Lee C et al (2012) Carbon nanotube-based membranes: fabrication and application to desalination. J Ind Eng Chem 18:1551–1559. doi:10.1016/j.jiec.2012.04.005
4. Dumee LF, Sears K, Schütz J et al (2010) Characterization and evaluation of carbon nanotube Bucky-Paper membranes for direct contact membrane distillation. J Memb Sci 351:36–43. doi:10.1016/j.memsci.2010.01.025

Giel *et al. Nanoscale Research Letters* (2017) 12:3

Page 14 of 15

5. Adams R, Carson C, Ward J et al (2010) Metal organic framework mixed matrix membranes for gas separations. Microporous Mesoporous Mater 131:13–20. doi:10.1016/j.micromeso.2009.11.035

6. Kusworo TD, Johari S, Widiasa IN (2012) The uses of carbon nanotubes mixed matrix membranes (MMM) for biogas purification. Int J Waste Resour 2:5–10. doi:10.12777/ijwr.v2i1.22

7. Sears K, Dumée L, Schütz J et al (2010) Recent developments in carbon nanotube membranes for water purification and gas separation. Materials (Basel) 3:127–149. doi:10.3390/ma3010127

8. Rezakazemi M, Ebadi A (2014) Progress in polymer science state-of-the-art membrane based CO_2 separation using mixed matrix membranes (MMMs): an overview on current status and future directions. Prog Polym Sci 39:817–861. doi:10.1016/j.progpolymsci.2014.01.003

9. Hashemifard SA, Ismail AF, Matsuura T (2011) Mixed matrix membrane incorporated with large pore size halloysite nanotubes (HNTs) as filler for gas separation: morphological diagram. Chem Eng J 172:581–590. doi:10.1016/j.cej.2011.06.031

10. Kusworo TD, Ismail AF, Widiasa IN, Johari S (2008) CO_2 removal from biogas using carbon nanotubes mixed matrix membranes. In: Proc. Int. Grad. Eng. Sci. pp 1–7

11. Wei Y, Shen L, Wang F et al (2011) Synthesis and characterization of novel nanocomposite membrane of sodium titanate/Nafion ®. Mater Lett 65:1684–1687. doi:10.1016/j.matlet.2011.02.081

12. Khan MM, Filiz V, Bengtson G et al (2012) Functionalized carbon nanotubes mixed matrix membranes of polymers of intrinsic microporosity for gas separation. Nanoscale Res Lett 7:1–12. doi:10.1186/1556-276X-7-504

13. Li Q, Zhang H, Tu Z et al (2012) Impregnation of amine-tailored titanate nanotubes in polymer electrolyte membranes. J Memb Sci 423–424:284–292, http://dx.doi.org/10.1016/j.memsci.2012.08.025

14. Robeson LM (2008) The upper bound revisited. J Memb Sci 320:390–400. doi:10.1016/j.memsci.2008.04.030

15. Li P, Wang Z, Qiao Z et al (2015) Recent developments in membranes for efficient hydrogen purification. J Memb Sci 495:130–168. doi:10.1016/j.memsci.2015.08.010

16. Lin R, Ge L, Hou L et al (2014) Mixed matrix membranes with strengthened MOFs/polymer interfacial interaction and improved membrane performance. Appl Mater Interfaces 6:5609–5618. doi:10.1021/am500081e

17. Slobodian P, Svoboda P, Kárászová M et al (2014) Carbon nanotube- and carbon fiber-reinforcement of ethylene-octene copolymer membranes for gas and vapor separation. Membranes (Basel) 4:20–39. doi:10.3390/membranes4010020

18. Mustafa A, Kusworo TD, Busairi A, Ismail AF (2012) Increasing the performance of PES-CNTs mixed matrix membrane using carbon nanotubes (CNTs) functionalization. Int J Waste Resour 2:22–24

19. Krishnamurthy G, Agarwal S (2013) Efficient synthesis of carbon nanotubes with improved surface area by low-temperature solvothermal route from dichlorobenzene. Chem Pap 67:1396–1403. doi:10.2478/s11696-013-0397-6

20. Wang S, Liu Y, Huang S et al (2014) Pebax-PEG-MWCNT hybrid membranes with enhanced CO_2 capture properties. J Memb Sci 460:62–70. doi:10.1016/j.memsci.2014.02.036

21. Surya Murali R, Sridhar S, Sankarshana T, Ravikumar YVL (2010) Gas permeation behavior of pebax-1657 nanocomposite membrane incorporated with multiwalled carbon nanotubes. Ind Eng Chem Res 49:6530–6538. doi:10.1021/ie9016495

22. Rajabi Z, Moghadassi AR, Hosseini SM, Mohammadi M (2013) Preparation and characterization of polyvinylchloride based mixed matrix membrane filled with multi walled carbon nano tubes for carbon dioxide separation. J Ind Eng Chem 19:347–352. doi:10.1016/j.jiec.2012.08.023

23. Kim S, Pechar TW, Marand E (2006) Poly(imide siloxane) and carbon nanotube mixed matrix membranes for gas separation. Desalination 192:330–339. doi:10.1016/j.desal.2005.03.098

24. Li X, Ma L, Zhang H et al (2015) Synergistic effect of combining carbon nanotubes and graphene oxide ins mixed matrix membranes for efficient CO_2 separation. J Memb Sci 479:1–10, http://dx.doi.org/10.1016/j.memsci.2015.01.014

25. Cong H, Zhang J, Radosz M, Shen Y (2007) Carbon nanotube composite membranes of brominated poly(2,6-diphenyl-1,4-phenylene oxide) for gas separation. J Memb Sci 294:178–185. doi:10.1016/j.memsci.2007.02.035

26. Liu R, Yang W, Chueng H, Ren B (2015) Preparation and application of titanate nanotubes on dye degradation from aqueous media by UV irradiation. J Spectrosc. 1–9. doi: 10.1155/2015/680183

27. Rodrigues CM, Ferreira OP, Alves OL (2010) Interaction of sodium titanate nanotubes with organic acids and base: chemical, structural and morphological stabilities. J Braz Chem Soc 21:1341–1348

28. Nada A, Moustafa Y, Hamdy A (2014) Improvement of titanium dioxide nanotubes through study washing effect on hydrothermal. Br J Environ Sci 2:29–40

29. Králová D, Grinevich A, Šlouf M (2009) Preparation of titanate nanotubes and their surface modification by plasma polymerization. 3:2008–2009. doi: 10.3217/978-3-85125-062-6-559

30. Giel V, Galajdová B, Popelková D et al (2015) Gas transport properties of novel mixed matrix membranes made of titanate nanotubes and PBI or PPO. Desalin Water Treat 56:3285–3293. doi:10.1080/19443994.2014.981931

31. Yang T, Chung T-S (2013) High performance ZIF-8/PBI nano-composite membranes for high temperature hydrogen separation consisting of carbon monoxide and water vapor. Int J Hydrogen Energy 38:229–239. doi:10.1016/j.ijhydene.2012.10.045

32. Weng TH, Tseng HH, Wey MY (2011) Effect of SBA-15 texture on the gas separation characteristics of SBA-15/polymer multilayer mixed matrix membrane. J Memb Sci 369:550–559. doi:10.1016/j.memsci.2010.12.039

33. Zhuang GL, Tseng HH, Wey MY (2014) Preparation of PPO-silica mixed matrix membranes by in-situ sol-gel method for H_2/CO separation. Int J Hydrogen Energy 39:17178–17190. doi:10.1016/j.ijhydene.2014.08.050

34. Sadeghi M, Semsarzadeh MA, Moadel H (2009) Enhancement of the gas separation properties of polybenzimidazole (PBI) membrane by incorporation of silica nano particles. J Memb Sci 331:21–30. doi:10.1016/j.memsci.2008.12.073

35. Shi C, Deng C, Zhang X, Yang P (2013) Synthesis of highly water-dispersible polydopamine-modified multiwalled carbon nanotubes for matrix-assisted laser desorption/ionization mass spectrometry analysis. ACS Appl Mater Interfaces 5:7770–7776. doi:10.1021/am4024143

36. Kim SW, Kim T, Kim YS et al (2012) Surface modifications for the effective dispersion of carbon nanotubes in solvents and polymers. Carbon N Y 50:3–33. doi:10.1016/j.carbon.2011.08.011

37. Jiang Y, Lu Y, Zhang L et al (2012) Preparation and characterization of silver nanoparticles immobilized on multi-walled carbon nanotubes by poly(dopamine) functionalization. J Nanoparticle Res 14:1–10. doi:10.1007/s11051-012-0938-x

38. Hebbar RS, Isloor AM, Ananda K, Ismail AF (2016) Fabrication of polydopamine functionalized halloysite nanotube/polyetherimide membranes for heavy metal removal. J Mater Chem A 4:1764–1774. doi:10.1039/C5TA09281G

39. Wan O, Tian J, Liu M et al (2015) Surface modification of carbon nanotubes via combination of mussel inspired chemistry and chain transfer free radical polymerization. Appl Surf Sci 346:335–341. doi:10.1016/j.apsusc.2015.04.012

40. Hu H, Yu B, Ye Q et al (2010) Modification of carbon nanotubes with a nanothin polydopamine layer and polydimethylamino-ethyl methacrylate brushes. Carbon N Y 48:2347–2353. doi:10.1016/j.carbon.2010.03.014

41. Rouquerolt J, Avnir D, Fairbridge CW et al (1994) Recommendations for the characterization of porous solids. Pure Appl Chem 66:1739–1758. doi:10.1351/pac199466081739

42. Williams MMR (1977) The mathematics of diffusion. Ann Nucl Energy 4:205–206. doi:10.1016/0306-4549(77)90072-X

43. Stuart B (2004) Infrared spectroscopy: fundamentals and applications. doi:10.1002/0470011149

44. Coates J (2000) Interpretation of infrared spectra, a practical approach interpretation of infrared spectra, a practical approach. In: Encycl. Anal. Chem. John Wiley & Sons Ltd, Chichester, pp 10815–10837

45. Chung TS, Guo WF, Liu Y (2006) Enhanced Matrimid membranes for pervaporation by homogenous blends with polybenzimidazole (PBI). J Memb Sci 271:221–231. doi:10.1016/j.memsci.2005.07.042

46. Paul DR (1979) Gas sorption and transport in glassy polymers. Berichte der Bunsengesellschaft für Phys Chemie 83:294–302. doi:10.1002/bbpc.19790830403

47. Chowdhury G, Kruczek B, Matsuura T (2001) Polyphenylene oxide and modified polyphenylene oxide membranes: gas. Vapor and Liquid Separation. doi:10.1007/978-1-4615-1483-1

48. Mittal V (2015) Manufacturing of nanocomposites with engineering plastics. doi:10.1016/B978-1-78242-308-9.09993-6

49. Sharma A, Tripathi B, Vijay YK (2010) Dramatic improvement in properties of magnetically aligned CNT/polymer nanocomposites. J Memb Sci 361:89–95. doi:10.1016/j.memsci.2010.06.005

50. Jiang LY, Huang Y, Jiang H et al (2006) A cohesive law for carbon nanotube/polymer interfaces based on the van der Waals force. J Mech Phys Solids 54:2436–2452. doi:10.1016/j.jmps.2006.04.009

51. Mahajan R, Koros WJ (2002) Mixed matrix membrane materials with glassy polymers. Part 1. Polym Eng Sci 42:1420–1431

52. Mahajan R, Koros WJ (2000) Factors controlling successful formation of mixed-matrix gas separation materials. Ind Eng Chem Res 39:2692–2696. doi:10.1021/ie990799r

53. Matteucci S, Yampolskii Y, Freeman BD, Pinnau I (2006) Transport of gases and vapors in glassy and rubbery polymers. In: Mater. Sci. Membr. Gas Vap. Sep. John Wiley & Sons, Ltd, Chichester, pp 1–47

54. Tena A, Marcos-Fernández A, Lozano AE et al (2013) Thermally segregated copolymers with PPO blocks for nitrogen removal from natural gas. Ind Eng Chem Res 52:4312–4322. doi:10.1021/ie303378k

55. Ismail AF, Khulbe K, Matsuura T (2015) Gas separation membranes—polymeric and inorganic. doi:10.1007/978-3-319-01095-3

56. Khan MM, Filiz V, Bengtson G et al (2013) Enhanced gas permeability by fabricating mixed matrix membranes of functionalized multiwalled carbon nanotubes and polymers of intrinsic microporosity (PIM). J Memb Sci 436: 109–120. doi:10.1016/j.memsci.2013.02.032

57. Ge L, Zhu Z, Rudolph V (2011) Enhanced gas permeability by fabricating functionalized multi-walled carbon nanotubes and polyethersulfone nanocomposite membrane. Sep Purif Technol 78:76–82. doi:10.1016/j.seppur.2011.01.024

58. Freeman BD, Carolina N (1999) Basis of permeability/selectivity tradeoff relations in polymeric gas separation membranes. Macromolecules 32:375–380. doi:10.1021/ma9814548

59. Paul D, Koros WJ (1976) Effect of partially immobilizing sorption on permeability and the diffusion time lag. J Polym Sci Polym Phys Ed 14:675–685. doi:10.1002/pol.1976.180140409

60. Wang R, Cao C, Chung T (2002) A critical review on diffusivity and the characterization of diffusivity of 6FDA – 6FpDA polyimide membranes for gas separation. J Memb Sci 198:259–271. doi:10.1016/S0376-7388(01)00665-2

61. Koros WJ, Chan AH, Paul DR (1977) Sorption and transport of various gases in polycarbonate. J Memb Sci 2:165–190, http://dx.doi.org/10.1016/S0376-7388(00)83242-1

62. Kim S, Chen L, Johnson JK, Marand E (2007) Polysulfone and functionalized carbon nanotube mixed matrix membranes for gas separation: theory and experiment. J Memb Sci 294:147–158. doi:10.1016/j.memsci.2007.02.028

63. Lin R, Ge L, Liu S et al (2015) Mixed-matrix membranes with metal–organic framework-decorated CNT fillers for efficient CO2 separation. ACS Appl Mater Interfaces 7:14750–14757. doi:10.1021/acsami.5b02680